ERDC/GRL MP-20-1

US Army Corps
of Engineers®
Engineer Research and
Development Center

An Airborne Lidar Point Cloud-based Below-Canopy Line-of-Sight Visibility Estimator

Heezin Lee, S. Bruce Blundell, Michael J. Starek,
and John G. Harris

January 2020

Geospatial Research Laboratory

The U.S. Army Engineer Research and Development Center (ERDC) solves the nation's toughest engineering and environmental challenges. ERDC develops innovative solutions in civil and military engineering, geospatial sciences, water resources, and environmental sciences for the Army, the Department of Defense, civilian agencies, and our nation's public good. Find out more at www.erdc.usace.army.mil.

To search for other technical reports published by ERDC, visit the ERDC online library at http://acwc.sdp.sirsi.net/client/default.

ERDC/GRL MP-20-1
January 2020

An Airborne Lidar Point Cloud-based Below-Canopy Line-of-Sight Visibility Estimator

Heezin Lee

National Center for Airborne Laser Mapping
Department of Earth and Planetary Science
University of California-Berkeley
Berkeley, CA 94720

S. Bruce Blundell

U.S. Army Engineer Research and Development Center
Geospatial Research Laboratory
7701 Telegraph Road
Alexandria, VA 22315

Michael J. Starek

Harte Research Institute for Gulf of Mexico Studies
Texas A&M University-Corpus Christi
Corpus Christi, TX 78412

John G. Harris

Department of Electrical and Computer Engineering
University of Florida
Gainesville, FL 32611

Final report

Prepared for U.S. Army Corps of Engineers
Washington, DC 20314-1000

Under DLET/IBFE; 4G18D6

Abstract

Point cloud data collected by small-footprint lidar scanning systems have proven effective in modeling the forest canopy for extraction of tree parameters. Although line-of-sight visibility (LOSV) in complex forests may be important for military planning and search-and-rescue operations, the ability to estimate LOSV from lidar scanners is not well-developed. A new estimator of below-canopy LOSV (BC-LOSV) by addressing the problem of estimation of lidar under-sampling of the forest understory is created. Airborne and terrestrial lidar scanning data were acquired for two forested sites in order to test a probabilistic model for BC-LOSV estimation solely from airborne lidar data. Individual crowns were segmented, and allometric projections of the probability model into the lower canopy and stem regions allowed the estimation of the likelihood of the presence of vision-blocking elements for any given LOSV vector. Using terrestrial lidar scans as ground truth, we found an approximate average absolute difference of 20% between BC-LOSV estimates from the airborne and terrestrial point clouds, with minimal bias for either over- or underestimates. The model shows the usefulness of a data-driven approach to BC-LOSV estimation that depends only on small-footprint airborne lidar point cloud and physical knowledge of tree phenology.

Contents

Abstract ii

Figures and Tables iv

Preface v

1 Introduction 1

2 Study Areas and Data Collection 2

3 Methods 4

3.1 Ground contribution to P(B) 4
3.2 Foliage contribution to P(B) 4
3.3 Tree stem contribution to P(B) 5
3.4 Calculation of BC-LOSV 6

4 Results and Discussion 8

5 Conclusion 10

References 11

Report Documentation Page

Figures and Tables

Figures

Figure 1. (a) Photos illustrating general scenes about the study areas for Site 1 (left) and Site 2 (right). (b) Concept of a BC-LOSV scope function, *S*, between the observer, *O*, and the target, *T*, showing terrestrial lidar points. 2

Figure 2. The difference in LOSV values (Y-axis) estimated from airborne and terrestrial data for Site 1, (a), and Site 2, (b), using a 1 m target. X-axis represents the indexed target locations. The outer green lines are the bounds 2X the average absolute LOSV difference. 8

Tables

Table 1. Average absolute difference in LOSV for three target sizes..... 8

Preface

This study was originally conducted for the Geospatial Research Laboratory under project 4G18D6, "DLET/IBFE" (completed FY14). The technical monitor was Mr. Nathan Frantz.

The project was executed by the Data and Signature Analysis Branch (TRS) of the TIG Research Division (TR), Army Engineer Research and Development Center, Geospatial Research Laboratory (ERDC-GRL). At the time of publication of this Miscellaneous Paper, Ms. Jennifer L. Smith was Chief, Data Signature and Analysis Branch (CEERD-TRS); Ms. Martha Kiene was Chief, TIG Research Division (CEERD-TR); and Mr. Ritchie Rodebaugh was Director of the Technical Directorate (CEERD-TET). The Deputy Director of ERDC-GRL was Ms. Valerie L. Carney and the Director was Mr. Gary Blohm.

COL Teresa A. Schlosser was Commander of ERDC, and Dr. David W. Pittman was the Director.

This work was supported by the U.S. Army Research Office (ARO) under Grant W911NF-06-1-0459. The authors would like to thank Dr. Ahmed Mohamed, Adam Benjamin, and Dr. Ben Wilkinson at the University of Florida for providing facilities and support during the collection of terrestrial lidar data.

1 Introduction

Airborne lidar scanning systems have found wide applicability for forest structure analysis (Maltamo et al. 2005; Chen et al. 2007; Palminteri et al. 2012). The portion of laser energy that reaches the ground can be used to estimate bare-surface topography (Reutebuch et al. 2003; Slatton et al. 2007; Carter et al. 2007), necessary to create a canopy height model (CHM) showing vegetation heights above the ground. The distribution of lidar return points in the forest column may also be used to estimate the sky-to-ground attenuation of visible light (Slatton et al. 2005; Lee et al. 2009). In spite of these advances, it has not yet been demonstrated that below-canopy line-of-sight visibility (BC-LOSV) can be robustly estimated from standalone airborne scanners where LOSV refers to the mutual visibility between two pairs of points in a terrain scene. The ability to model lateral viewing under the trees and the probable locations of vision-blocking elements for a particular forest stand can be important for military planning and search-and-rescue operations.

Estimation of lateral visibility in forests is difficult because the foliage of the upper layer of the forest canopy (tree crowns) acts as a collection of blocking elements that can occlude all or a portion of the laser pulse from further penetration. This can result in lidar under-sampling of the lower portion of the canopy, tree stems, and understory. In this work, we pursue a formal estimation of under-sampling probabilities from the lidar point cloud as a function of canopy depth and structure.

2 Study Areas and Data Collection

This study was conducted at the Austin Carey Memorial Forest (ACMF) located 15km northeast of Gainesville, Florida and managed by the School of Forest Resources and Conservation of the University of Florida. Two study sites were chosen, about 200 meters apart, each site enclosing an area of 60 m x 80 m. The topography in these sites is relatively flat, with ground elevations varying as little as 1.5 m. Forest composition is similar for both sites, though Site 2 has much denser understory than Site 1. The overstory consists of longleaf pine and slash pine, and the understory is dominated by saw palmetto, gallberry, wax myrtle, and wiregrass (Powell et al. 2008). A general scene for each site is shown in Figure 1(a).

Figure 1. (a) Photos illustrating general scenes about the study areas for Site 1 (left) and Site 2 (right). (b) Concept of a BC-LOSV scope function, *S*, between the observer, *O*, and the target, *T*, showing terrestrial lidar points.

(a)

(b)

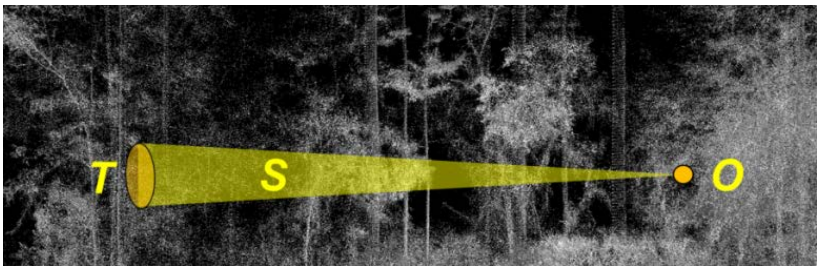

The study area was scanned by Kucera International, Inc. with a 200 kHz Leica ALS60 discrete-return airborne lidar system in midwinter 2011. Each of the two sites was imaged with four flight lines, one for each of the four cardinal directions from an altitude of 1200 m. The average lidar point density at both sites was approximately 17.0 point/m^2 (average point spacing = 0.24 m). Terrestrial lidar scanning was also performed at each site within a few days of the aerial overflights with a Leica ScanStation 2 system. This terrestrial point cloud model served to verify the BC-LOSV estimation from the airborne data. Seven scans were acquired at Site 1 and eleven scans at Site 2 and co-registered to generate a contiguous 3D model

of the forest. The average lidar point density was 2721.5 points/m^2 at Site 1 and 6192.4 points/m^2 at Site 2.

3 Methods

Our approach to estimating lateral visibility under the canopy involved discretizing the 3D space of the point cloud into voxels and estimating the probability of occlusion or blockage $P(B|X=x_i, Y=y_i, Z=z_i)$ on a voxel-by-voxel basis. We set the voxel size to 0.1 m × 0.1 m × 0.1 m, and each voxel was assigned a probability from 1 (complete blockage) to 0 (no blockage). This will allow a line-of-sight computation between any two points in the 3D space having a particular direction and range. Contributions to the probability of blockage $P(B)$ for each voxel come from (1) the ground, (2) the foliage, and (3) the tree stems.

3.1 Ground contribution to P(B)

For the ground contribution, [$P_{ground}(B)$], we first estimated a bare-earth DEM with decimeter accuracy by segmentation and interpolation of ground points. Filtering is applied to remove non-ground points (Kampa and Slatton, 2004), and the points are then interpolated by Kriging into bare-earth elevation grids at a desired spatial resolution (here, 1m). The bare-earth model acted as a lower boundary constraint on LOSV. Complete vision blockage is assigned to all voxels below and touching the surface [$P_{ground}(B) = 1$], with the rest of the voxels tagged as having no blockage [$P_{ground}(B) = 0$].

3.2 Foliage contribution to P(B)

We then considered the contributions by foliage and branches of the canopy and understory vegetation, [$P_{foliage}(B)$], represented by the set of non-ground lidar points. The set of non-ground points was generated directly from the ground point filtering process described in Section 3.1 above. Given that the size of the lidar footprint is 15-20 cm, we assigned complete blockage to a voxel [$P_{foliage}(B) = 1$] if there is at least one lidar point inside 10 cm from the center of the voxel. Because the lidar point density in the lower canopy and understory is progressively less representative of vegetation due to attenuation of available lidar pulses in the forest column, we employed a sampling strategy using monotonically decreasing sets of points as a function of elevation from canopy top to ground level. This is added to the probability of occlusion due to directly observed points.

The estimated foliage by the sampling method, $[P_{foliage}(B)]_{estimated}$, is developed in the following way. A narrow cylinder channel of 0.5 m radius is inscribed around each voxel from the top of the canopy to the ground. All lidar points inside the channel are used to estimate the vegetation density for the enclosed voxel. Since there is often little or no information between the crown base and the ground, we made the simple assumption that the vegetation medium inside the channel is uniformly distributed, and therefore the decrease in density of the non-ground lidar points from canopy top to ground must be monotonic.

We define $[P_{foliage}(B)]_{estimated}$ for a voxel as the product of the vegetation medium density inside the channel (D_{veg}) and the estimated lidar point density in a small local region near the voxel (D_{local}). D_{veg} is the number of non-ground points in the channel as a fraction of the total number of points in the channel. We then define the estimated local point density D_{local} as the ratio of the distance-weighted sum of the number of points near the voxel to the distance-weighted number of non-ground points. The weights applied to each point are given by the fractional distance from the top of the canopy.

3.3 Tree stem contribution to P(B)

We now turn to the final contribution to $P(B)$ from tree stems. Though poorly sampled by airborne lidar, they will strongly affect BC-LOSV. We derived stem characteristics by first extracting their corresponding tree crowns in a two-stage process: the top-level crown structure followed by the understory. We used an adaptive clustering algorithm, previously tested in managed pine forests (Lee et al. 2010) to segment individual top-level tree crowns. To segment the understory crowns, a spin image (Johnson and Hebert 1999; Caceres and Slatton 2007) of size 3 m x 5 m was computed for each individual point in the remaining understory cloud starting from the highest point. When this technique is applied to a tree canopy point cloud, the result is a distribution of binned points in the image spreading diagonally from upper left to lower right. Principal Components Analysis (PCA) (Fukunaga 1999) was applied to each spin image to check the existence of the diagonal structure of understory canopies. To be a tree cluster, it was assumed that the first principal component contains most of the variance (90%). In addition, the axis with the largest variance should reside in the second and fourth quadrants in the spin image space, since the distributions of tree clusters are from the upper left to the lower right.

Once all the individual trees are segmented, we estimate certain parameters such as tree height (*TH*) and crown diameter (*CD*) for the segmented points. Using these values for each tree, existing allometric equations can be applied to estimate the likely range of stem diameter at breast height, D_{bh}, for common tree species. To this end, we applied the stochastic relation developed by Popescu (Popescu 2007) (Equation 1).

$$D_{bh} = -0.16 + CD + 1.22 \times TH \tag{1}$$

TH is measured from the highest point in each segmented tree to the ground surface. *CD* is computed directly from crown area, which is derived from a convex hull inscribed around the segmented area for each tree. Linear regression of D_{bh} estimates in the study (Popescu, 2007) indicated an RMSE of approximately 20% of average D_{bh} for all measured trees. The stem diameters, together with 20% uncertainty, enable us to relate stem contributions to *P(B)* as shown by Equation 2, where d_{vt} is the horizontal distance from voxel center to tree location.

$$P_{stem}(B) = \begin{cases} 1 & \left(0 \le d_{vt} \le D_{bh}\right) \\ 0.8 & \left(D_{bh} \le d_{vt} \le 1.2 D_{bh}\right) \end{cases} \tag{2}$$

3.4 Calculation of BC-LOSV

To determine the blockage between an observer and a target, an optical scope function is defined originating at the observer and extending through the vegetation in the direction of the target. The scope function (Figure 1b) was chosen to be a second-order polynomial to model the optical property that an object's occluding effect becomes less sensitive to changes in its distance from the observer as the distance increases. We assumed the targets to be a circle with a diameter of one meter.

The probability of blockage between the observer, *O,* and target, *T*, in a forest is determined as a sum of the discretized probability of blockage values from ground, foliage, and tree stems contained within the line-of-sight scope function *S*, for a particular field-of-view and range between *O* and *T* where $(i, j, k) \in S$ (Eq. 3). Then the LOSV for a particular scope function equals one minus the probability of blockage and ranges from zero to one.

$$P(B)_{(O,T)} = \sum_{i,j,k}\left[P_{ground}\left(B|x_i, y_j, z_k\right) + P_{foliage}\left(B|x_i, y_j, z_k\right) + P_{stem}\left(B|x_i, y_j, z_k\right)\right] \quad (3)$$

In order to verify $P(B)_{(O,T)}$, we placed a hypothetical observer in each site at a height of 1.5 m under the forest canopy at the center of a square box 40 m on a side. The box was positioned near the center of each site. We then located a total of 160 hypothetical targets at the same height as the observer on the periphery of each box at 1 m intervals. The distance between the observer and the targets ranges from 20 m to 28.3 m.

4 Results and Discussion

To verify the below-canopy blockage model, the LOSV estimated from the airborne point clouds is compared to that computed from the terrestrial point clouds. Final results for the difference of LOSV estimated from airborne and terrestrial point clouds at each site are given in Figure 2. In each graphic, the difference of LOSV is shown for 160 hypothetical target locations located around the periphery of the observer's "box" positioned at each site. The average absolute difference in LOSV is 0.202 for Site 1 and 0.182 for Site 2, i.e. the error in the estimates at both sites is about 20%. These results imply that the LOSV derived from airborne point clouds are in reasonably good agreement with ground truth as represented by the terrestrial point cloud, although it is possible for larger local errors to occur. Interestingly, the difference in estimation accuracy between the two sites is quite small and non-significant (based on a t-test) even though Site 2 has much denser understory. As the target diameter is increased, the average absolute difference in LOSV decreases and a similar agreement in performance between sites is maintained (Table 1).

Figure 2. The difference in LOSV values (Y-axis) estimated from airborne and terrestrial data for Site 1, (a), and Site 2, (b), using a 1 m target. X-axis represents the indexed target locations. The outer green lines are the bounds 2X the average absolute LOSV difference.

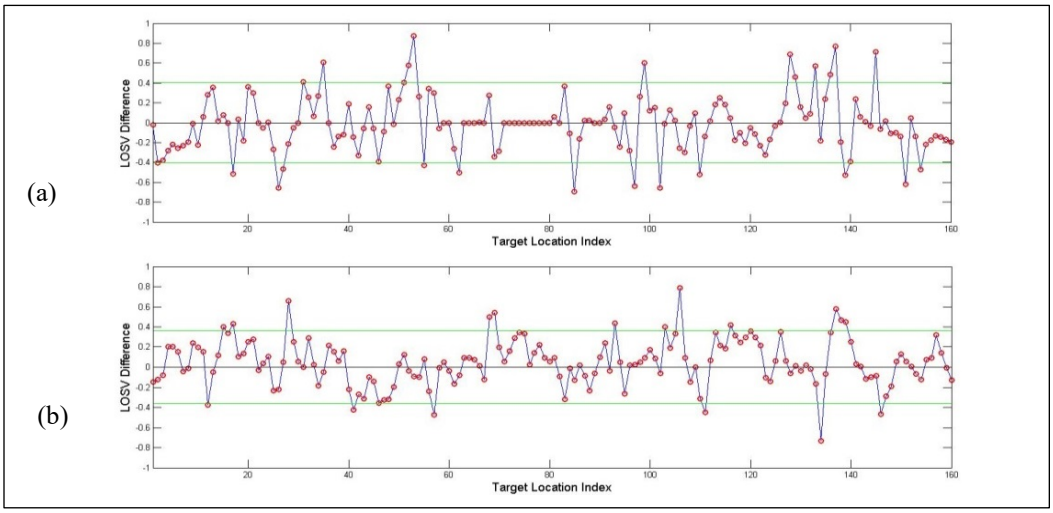

Table 1. Average absolute difference in LOSV for three target sizes.

	Target Size (diameter)		
	1m	2m	3m
Site #1	0.202	0.172	0.169
Site #2	0.182	0.166	0.157

Differences at each target location between LOSV estimated from the airborne and terrestrial point clouds can be one of two types: overestimation or underestimation. Using a minimum threshold of 2X the average absolute LOSV difference for each site, target locations with outlier LOSV difference values may be determined. For site 1, there are a total of 24 instances of LOSV differences above the threshold, 12 outlier differences are overestimates (positive) and 12 are underestimates (negative). Site 2 has a total of 21 outliers, 10 overestimates and 11 underestimates.

In the case of the LOSV underestimates, the terrestrial point cloud generally shows very little blocking vegetation, so that the probability model overestimates the vegetation medium density in the channel and/or falsely locates tree stems. Overestimation is mainly due to the lack of sufficient lidar penetration into the upper canopy, resulting in insufficient availability of information for a proper estimation of vegetation density.

In order to verify our model for LOSV, we used terrestrial lidar point clouds as quasi-ground truth. However, there are several sources of potential discrepancies between this ground truth and the real world. It is unknown how close the registered terrestrial point cloud data represent the details of actual complex forests. However, we believe that our scans capture the major structure of the forest sites in this study. There was also some registration error (about 12 cm) between the terrestrial and airborne data sets, and this error could affect results because our targets are small and the cone used in the scope function is narrow. Slight shifts in the LOSV results could be due to this error. Other sources of error, though likely small, include the difference in survey time between the terrestrial data (collected over three days) and the airborne data (collected over one day), and local disruptions over this time period from animals, forest managers, and wind.

Tree stems play a major role in blocking line-of-sight, but detecting their exact locations from airborne lidar sensors is a challenging problem. Treetops may deviate from ground stem locations in the x-y plane. Future work may include looking for a relationship between this deviation and species or crown shape, for example.

5 Conclusion

In this work, we have shown that it is possible to estimate BC-LOSV at any location in the forest environment using airborne lidar data in a manner that is more accurate and generalized than has been possible to date. Dense ground-based lidar data were collected to validate the BC-LOSV estimates. Our airborne lidar-derived estimates were in reasonably good average agreement with the BC-LOSV computed from terrestrial lidar. Our proposed approach allows prediction of LOSV for skyward as well as lateral viewing.

This project was designed to further the understanding and application of lidar data to the forest environment to enhance military and civil capabilities in assessing under-canopy terrain, line-of-sight, and mobility. The estimation of *P(B)* statistically characterizes the clutter environment. This represents useful information in developing detection algorithms for targets under the canopy, regardless of whether they are intended for lidar, radar, or thermal IR sensing.

References

Caceres, J.J. and K. C. Slatton. 2007. Improved classification of building infrastructure from airborne lidar data using spin images and fusion with ground-based lidar, *IEEE/ISPRS Urban Remote Sensing Joint Event*, April, 2007, pp. 1-7.

Carter, W.E., R.L. Shrestha, and K.C. Slatton. 2007. Geodetic laser scanning, *Physics Today*, December 2007.

Chen, Q., P. Gong, D. Baldocci, and Y.Q. Tian. 2007. Estimating basal area and stem volume for individual trees from lidar data, *Photogrammetric Engineering and Remote Sensing,* 73(12):1355-1365.

Fukunaga, K. 1999. *Introduction to Statistical Pattern Recognition*, Academic Press, New York.

Johnson, A.E. and M. Hebert. 1999. Using spin images for efficient object recognition in cluttered 3D scenes, *IEEE Transactions on Pattern Analysis and Machine Intelligence,* 21(5):433-449.

Kampa, K., and K.C. Slatton. 2004. An adaptive multiscale filter for segmenting vegetation in ALSM data, *IEEE Geoscience and Remote Sensing Symposium (IGARSS)*, 6:3837-3840.

Lee, H., K.C. Slatton, B. Roth, and W.P. Cropper. 2009. Prediction of forest canopy sunlight interception using three-dimensional airborne data, *International Journal of Remote Sensing,* 30(1):189-207.

Lee, H., K.C. Slatton, B. Roth, and W.P. Cropper. 2010. Adaptive clustering of airborne lidar data to segment individual tree crowns in managed pine forests, *International Journal of Remote Sensing,* 31(1):117-139.

Maltamo, M., K. Eerikainen, J. Hyppa, J. Pitkanen, P. Packalen, and X. Yu. 2005. Identifying and quantifying structural characteristics of heterogeneous boreal forests using laser scanning data, *Forest Ecology and Management,* 216(1-3):41-50.

Palminteri, S., G.V. Powell, G.P. Asner, and C.A. Peres. 2012. Lidar measurements of canopy structure predict spatial distribution of a tropical mature forest primate, *Remote Sensing of Environment*, 127:98-105

Popescu, S.C. 2007. Estimating biomass of individual pine trees using airborne lidar, *Biomass and Bioenergy,* 31:646-655.

Powell, T.L., H.L. Gholz, K.L. Clark, G. Starr, W.P. Cropper, and T.A. Martin. 2008. Carbon exchange of a naturally-regenerated pine forest in north Florida, *Global Change Biology,* 14:2523-2538.

Reutebuch, S.E., R.J. McGaughey, H. Andersen, and W.W. Carson. 2003. Accuracy of a high-resolution lidar terrain model under a conifer forest canopy, *Canadian Journal of Remote Sensing,* 29(5):527-535.

Slatton, K. C., W. E. Carter, R. L. Shrestha, and W. Dietrich. 2007. Airborne Laser Swath Mapping: Achieving the resolution and accuracy required for geosurficial research, *Geophysical Research Letters,* 34, L23S10, doi:10.1029/2007GL031939.

Slatton, K.C., H. Lee, K. Kampa, and H. Jhee. 2005. Segmentation of ALSM point data and the prediction of subcanopy sunlight distribution, *Proceedings of the IEEE 2005 International Geoscience and Remote Sensing Symposium (IGARSS),* 1:525-528.

REPORT DOCUMENTATION PAGE

Form Approved
OMB No. 0704-0188

1. REPORT DATE *(DD-MM-YYYY)*	2. REPORT TYPE	3. DATES COVERED *(From - To)*
January 2020	Final	

4. TITLE AND SUBTITLE

An Airborne Lidar Point Cloud-based Below-Canopy Line-of-Sight Visibility Estimator

5a. CONTRACT NUMBER

5b. GRANT NUMBER

5c. PROGRAM ELEMENT NUMBER

6. AUTHOR(S)

Heezin Lee, S. Bruce Blundell, Michael J. Starek, and John G. Harris

5d. PROJECT NUMBER
4G18D6

5e. TASK NUMBER

5f. WORK UNIT NUMBER

7. PERFORMING ORGANIZATION NAME(S) AND ADDRESS(ES) (see reverse)

8. PERFORMING ORGANIZATION REPORT NUMBER

ERDC/GRL MP-20-1

9. SPONSORING / MONITORING AGENCY NAME(S) AND ADDRESS(ES)

U.S. Army Corps of Engineers
Washington, DC 20314-1000

10. SPONSOR/MONITOR'S ACRONYM(S)

11. SPONSOR/MONITOR'S REPORT NUMBER(S)

12. DISTRIBUTION / AVAILABILITY STATEMENT

Approved for public release; distribution is unlimited.

13. SUPPLEMENTARY NOTES

Journal of Applied Remote Sensing, vol. 7, No. 1 September 5, 2013

14. ABSTRACT

Point cloud data collected by small-footprint lidar scanning systems have proven effective in modeling the forest canopy for extraction of tree parameters. Although line-of-sight visibility (LOSV) in complex forests may be important for military planning and search-and-rescue operations, the ability to estimate LOSV from lidar scanners is not well-developed. A new estimator of below-canopy LOSV (BC-LOSV) by addressing the problem of estimation of lidar under-sampling of the forest understory is created. Airborne and terrestrial lidar scanning data were acquired for two forested sites in order to test a probabilistic model for BC-LOSV estimation solely from airborne lidar data. Individual crowns were segmented, and allometric projections of the probability model into the lower canopy and stem regions allowed the estimation of the likelihood of the presence of vision-blocking elements for any given LOSV vector. Using terrestrial lidar scans as ground truth, we found an approximate average absolute difference of 20% between BC-LOSV estimates from the airborne and terrestrial point clouds, with minimal bias for either over- or underestimates. The model shows the usefulness of a data-driven approach to BC-LOSV estimation that depends only on small-footprint airborne lidar point cloud and physical knowledge of tree phenology.

15. SUBJECT TERMS

Lidar, canopy segmentation, tree parameters, line-of-sight visibility

16. SECURITY CLASSIFICATION OF:			17. LIMITATION OF ABSTRACT	18. NUMBER OF PAGES	19a. NAME OF RESPONSIBLE PERSON
a. REPORT	b. ABSTRACT	c. THIS PAGE			19b. TELEPHONE NUMBER *(include area code)*
Unclassified	Unclassified	Unclassified	SAR	21	

7. PERFORMING ORGANIZATION NAME(S) AND ADDRESS(ES) (concluded)

National Center for Airborne Laser Mapping
Department of Earth and Planetary Science
University of California-Berkeley
Berkeley, CA 94720

U.S. Army Engineer Research and Development Center
Geospatial Research Laboratory
7701 Telegraph Road
Alexandria, VA 22315

Harte Research Institute for Gulf of Mexico Studies
Texas A&M University-Corpus Christi
Corpus Christi, TX 78412

Department of Electrical and Computer Engineering
University of Florida
Gainesville, FL 32611